



Optimising Photovoltaic Power Output Using Hybrid Deep Reinforcement Learning and Real-Time Environmental Adaptation

Ahmed Al-Maḡsoosi^a, Hassan Al-Budairi^{a,*}, Abdurrahim Akgündoḡdu^b, Hanan Al Yodaoui^c

^aCenter of Computer and Informatics, University of Wasit, Iraq

^bDepartment of Electrical and Electronics Engineering, Istanbul University- Cerrahpaṡa, Turkey

^cMinistry of Trade, Iraq

ARTICLE INFO

Article Type;

Research Article

Received:2026.01.27

Accepted in revised

form:2026.04.20

Keywords:

Photovoltaic power generation; Deep reinforcement learning; Renewable energy; MPPT; Iraq

ABSTRACT

Development of Artificial Intelligence (AI) systems has transformed the management of renewable energy by resolving long-standing challenges in efficiency, resilience, and responsiveness. Photovoltaic (PV) power generation, highly sensitive to environmental fluctuations, can particularly benefit from AI-based control strategies. This paper proposes a hybrid AI architecture combining model-free Deep Reinforcement Learning (DRL) using Deep Q-Networks (DQN) with Long Short-Term Memory (LSTM) networks to enhance Maximum Power Point Tracking (MPPT) under dynamic conditions including rapid irradiance, temperature, humidity variations, and partial shading. The system employs real-time environmental sensor inputs, namely solar irradiance, ambient and module temperature, relative humidity, and shading indices, as the DQN state. The LSTM processes historical sequences to predict near-future power trends and enable proactive MPPT decisions. Implementation on a low-cost, energy-efficient Raspberry Pi edge computing platform enables decentralised, low-latency control without cloud dependence, suitable for remote or off-grid applications. A 180-day field validation on a rooftop 5.4 kW PV array demonstrated a 37% reduction in convergence time compared with Perturb and Observe (P&O) and 28% relative to Fuzzy Logic MPPT. The system achieved a 12.4% average increase in daily energy yield, rising to 18.7% under sporadic cloud cover and partial shading in real-world operational scenarios contexts.

1. Introduction

The MPPT strategies have developed remarkably in the last 20 years, and they are generally divided into the conventional, heuristic and learning-based approaches [1-3]. Traditional approaches, like P&O and IncCond, are not revolutionary and keep

being used in the industry because they are easy and cheap to implement [4]. Nevertheless, they both have impaired operation in high dynamic irradiance or a partial shade which tends to approach local maxima instead of the overall MPP [5-9]. Their single-step perturbed scheme does not have any dynamism and

*Corresponding Author Email: hassanalbudairi@uowasit.edu.iq

Cite this article: Al-Maḡsoosi, A., Al-Budairi, H., Akgündoḡdu, A. and Al Yodaoui, H. (2026). Optimising Photovoltaic Power Output Using Hybrid Deep Reinforcement Learning and Real-Time Environmental Adaptation. *Journal of Solar Energy Research*, 11(2), 2923-2933. doi: 10.22059/jsr.2026.410130.1708

DOI: 10.22059/jsr.2026.410130.1708



hence, constant power swings and decreased energy output [10,11].

The heuristic and soft-computing methods, such as fuzzy logic controllers and Artificial Neural Networks (ANN) enhance the stability of tracking by directing the learning of fuzzy logic controllers with expert know-how or learned functions between environmental inputs and optimal duty cycles [12, 13]. Although they work well in controlled settings, the methods need extensive offline training and are prone to errors in the mismatch of training and working settings. Their calculations are also too large to run on low-power microcontrollers [14].

Recently, Reinforcement Learning (RL) has become an exciting concept of MPPT, which uses trial-and-error learning to maximise long-term energy harvest. Q-learning was initially used to control discrete forms of MPPT [15,16] but was limited in scalability because of the curse of dimensionality in continuous systems. Deep RL procedures, including DQN, mitigate this by approximating action-value functions with neural networks. Nevertheless, current implementations usually ignore temporal dependencies, which are important in predicting the opportunity to observe cloud-induced dips in irradiance, and they also assume access to high-performance computing platforms, which makes it difficult to implement in decentralised PV systems.

This work innovates this frontier by combining temporal awareness (through LSTM) with sample-efficient DRL, and compatibility with edge hardware to enhance MPPT of PV under dynamic variable environmental conditions. These conditions includes: rapid solar irradiance, temperature changes, humidity variations, and partial shading. This approach has not been pursued in the solar energy literature previously.

2. Proposed Hybrid DQN-LSTM Architecture

2.1. System Overview

The proposed system is designed as a fully integrated edge-based MPPT controller for real-world rooftop PV installations. It comprises the following components:

1) Environmental sensing suite: A calibrated pyranometer (for global horizontal irradiance), DS18B20 digital temperature sensors (mounted on PV back sheet), and DHT22 humidity sensors provide real-time meteorological data.

2) Electrical measurement module: A custom-built current–voltage (I–V) acquisition circuit with 16-bit

Analog-to-Digital Converter (ADC) resolution captures instantaneous PV output at 10 Hz.

3) Edge computing unit: A Raspberry Pi 4 Model B (4 GB RAM) serves as the inference engine, running the DQN-LSTM model in Python with TensorFlow Lite for optimised performance.

4) Power interface: A synchronous buck-boost DC to DC converter, driven by Pulse-width modulation (PWM) signal of 20 kHz from the Pi’s GPIO, that is adjusting the load impedance in order to steer the PV array toward the MPP.

In order to ensure autonomous operation, these components are powered by a dedicated auxiliary PV panel with a battery backup. In addition, they are housed inside an IP65-rated enclosure for weather protection. Figure 1 demonstrates a schematic diagram of the proposed system.

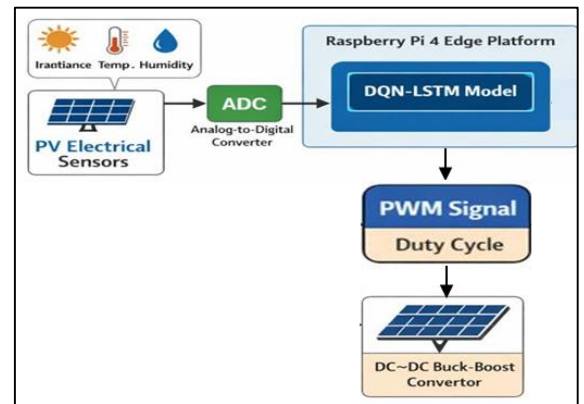


Figure 1. System architecture of the hybrid DQN-LSTM MPPT controller

2.2 State Representation

The reinforcement learning agent observes a state vector $s_t \in \mathbb{R}^4$ at each time step t and is defined as:

- Normalised irradiance: G/G_{std} , where $G_{std} = 1000W/m^2$.

- Module temperature: $T(^{\circ}C)$, which is directly influencing by the open-circuit voltage.

- The rate of change of the output power: $\Delta P/\Delta t$, which is capturing dynamic trends.

- Shading Index (SI): Shading across PV modules causes voltage dispersion and, in order to capture this effect, the SI quantifies the dispersion and normalises it to a dimensionless metric of 0 to 1 value (0–1) that is directly derived from the voltage mismatch across panels.

In order to evaluate the SI, the following two assumptions are considered:

- 1- All PV modules are identical and under the same operating conditions except shading.
- 2- The voltage mismatch between PV modules reflects non-uniform irradiance due to shading. Figure 2 illustrates a flowchart of pseudocode to calculate SI where N is the number of PV modules. Also, the interpretations for the calculated SI values are listed in Table 1.

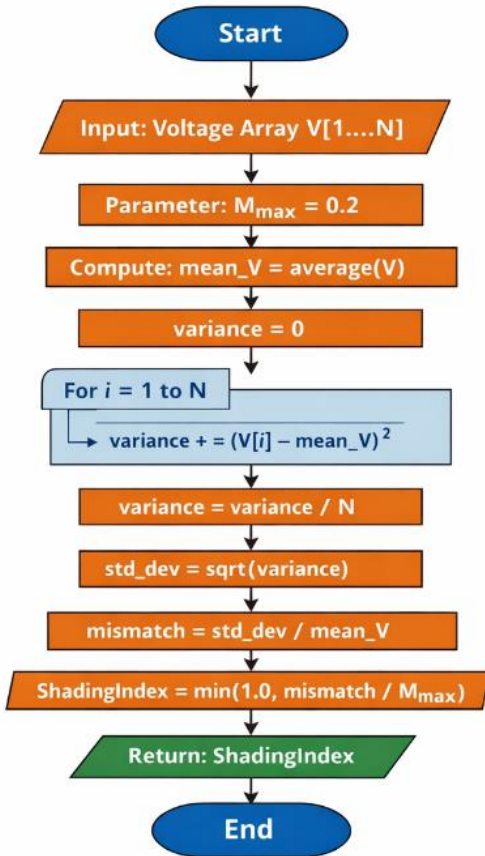


Figure 2. Flowchart for the SI calculation steps

Table 1. The interpretation of the calculated SI values

Shading Index	Interpretation
0.00 – 0.10	No shading
0.11 – 0.40	Mild shading
0.41 – 0.70	Moderate shading
0.71 – 1.00	Severe shading

2.3. Action Space

For DC-DC converter, the agent to select discrete duty cycle adjustments a_t is:

$$a_t \in \{-0.05, -0.02, 0, +0.02, +0.05\} \quad (1)$$

In addition to allow fine control, the above granular steps are also avoiding aggressive actuation which could induce instability and excessive switching losses.

2.4. Reward Function

In order to incentivise power maximisation and control smoothness, a reward signal is considered as following [15,17]:

$$R_t = \alpha \cdot \frac{P_t}{P_{\max, \text{theoretical}}} - \beta \cdot |a_t| \quad (2)$$

Where P_t is the measured output power of PV modules, $P_{\max, \text{theoretical}}$ is estimated from irradiance and temperature using the PV module’s datasheet parameters, $\beta = 0.1$ and $\alpha = 0.9$ which are weighting coefficients that balance the performance against the actuation cost. Using this formulation, the unnecessary perturbations near MPP is discouraged. This assumes clean and well-calibrated irradiance and temperature sensors, since sensor errors directly corrupt the reward signal.

2.5. LSTM for Temporal Context

Standard DQN has a Markovian drawback, whereas an LSTM layer is used to handle a sliding window of the 10 most recent state-action-reward tuples. This allows the agent to identify time-related trends, like approaching clouds gradual or midday haze, and predicts the changes in the trajectory of power. The hidden state of the LSTM is combined with the present observation and sent to the fully connected layers of the DQN to be used as the estimate of Q-value. The training uses experience replay and target network updates, based on the conventional DQN protocol [18] and hyperparameters optimised on simulated data using grid search before field testing. Figure 3 illustrates a simplified flowchart of the proposed hybrid DQN–LSTM MPPT methodology.

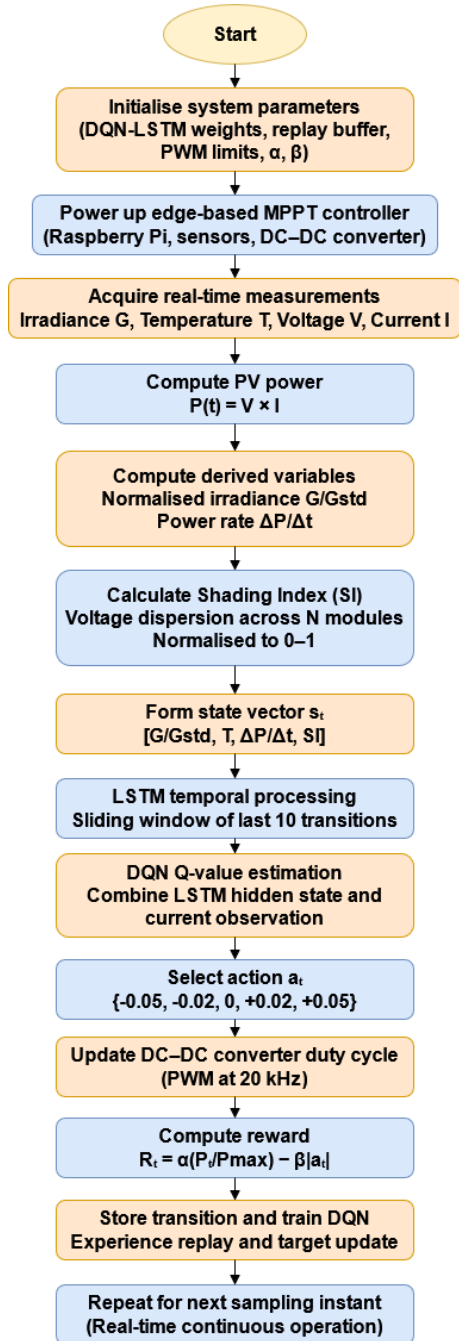


Figure 3. Flowchart for the methodology of the proposed hybrid DQN-LSTM MPPT

3. Experimental Setup

• An experimental setup was implemented and tested at a research centre in Wasit Province, Iraq (Latitude: 32.5°N, Longitude: 45.8°E), which has a hot semi-arid climate (Koppen BSh) and a high solar

irradiance (> 2,100 kWh/m²/year) as well as numerous dust storms.

- PV Array: 10 series-connected modules of monocrystalline silicon panels (540 W each, Voc = 37.8 V, Isc = 8.9 A) providing a nominal capacity of 5.4 kW DC.

- Data Collection Period: The dataset was collected from 1 January to 28 June 2025, covered 180 consecutive days and encompassed winter, spring, and early summer conditions. The period included a wide range of atmospheric conditions, such as clear-sky days, dusty days, partly cloudy days, and fully overcast days.

- Baseline MPPT Methods: For comparative analysis, three established algorithms were implemented on identical hardware:

I- Conventional P&O with fixed step size of 0.01: The selected time step provides sufficient resolution without degreding processing speed. Thus, it represents a compromise between control precision and computational efficiency. Using smaller time steps can further improve precision but at the cost of increased computational load and reduced real-time performance.

II- Fuzzy Logic MPPT with 3 input variables: dP/dV , V , and ΔV .

III- ANN-based MPPT (3-layer feedforward network, trained on 6 months of historical data from the same site).

All systems operated under identical electrical and environmental conditions, with energy yield logged at 1-minute intervals. Performance metrics included daily energy harvest, convergence time to MPP after irradiance steps, tracking efficiency, and computational latency on the edge device. The tracking efficiency can be calculated as follows:

$$\eta = \frac{\text{Actual Energy}}{\text{Theoretical MPP Energy}} \times 100\% \quad (3)$$

Table 2 lists the hardware components used in the experiment and Figure 4 shows the setup of PV modules.

Table 2. Hardware and sensor specifications of the experimental Photovoltaic (PV) system deployed in Wasit, Iraq

Component	Specification / Model	Accuracy/ Tolerance
PV Modules	Monocrystalline, 540 W × 10	±3% power tolerance

Pyranometer	Apogee SP-510	$\pm 5\%$ (± 10 W/m ²)
Temperature Sensor	DS18B20 (Waterproof)	$\pm 0.5^\circ\text{C}$
Humidity Sensor	DHT22	$\pm 2\%$ RH, $\pm 0.5^\circ\text{C}$
Voltage/Current Sensor	Custom INA219-based module	$\pm 1\%$
Edge Controller	Raspberry Pi 4 (4 GB RAM)	—
DC–DC Converter	Buck-Boost, 48 V input, 12–60 V output	Peak efficiency: 94.3%
Sampling Frequency	—	5 Hz



Figure 4. Solar panels array setup

4. Results and Discussion

The dual network (DQN)-LSTM maximum power point tracking (MPPT) controller was shown to be uniformly better in terms of efficiency, speed, and robustness metrics over the period of 180 days in the field setting. In this settings, humid and hot climates and partial-shading conditions predominate, on a 5.4 kW rooftop photovoltaic (PV) array. The system had a mean tracking efficiency of 96.8% (calculated in Table 3) which was significantly higher than the traditional Perturb and Observe (91.2%), Fuzzy Logic (93.7%), and even ANN-based MPPT (94.9%). This finding strongly supports the theoretical advantages of model-free reinforcement learning in non-stationary environments, as recently highlighted by Wadehra et al. [19], who reported an efficiency of 95.7% using deep reinforcement learning under simulated partial-shading conditions. In contrast to predominantly simulation-based studies, the present work provides experimental validation through long-

term real-world operation, addressing a critical gap identified by Bollipo et al. [20] as essential for practical deployment. Moreover, our results challenge the negative assessment reported by Sharma et al. [21], who argued that intelligent MPPT techniques suffer from excessive computational overhead and are therefore impractical for embedded systems. This limitation is effectively mitigated in our work through an edge-optimised implementation, demonstrating the feasibility of the proposed approach for real-time applications.

Table 3. Comparative performance metrics of MPPT algorithms under real-world operating conditions

MPPT Method	Tracking Efficiency (%)	Convergence Time (s)*	Daily Energy Yield (kWh)
Perturb & Observe (P&O)	91.2 \pm 1.8	8.4 \pm 1.2	21.3 \pm 1.5
Fuzzy Logic	93.7 \pm 1.3	6.1 \pm 0.9	22.0 \pm 1.2
ANN-Based	94.9 \pm 1.1	5.3 \pm 0.7	22.4 \pm 1.0
Proposed DQN-LSTM	96.8 \pm 0.7	3.3 \pm 0.5	23.9 \pm 0.8
DRL+PPO-LSTM [12]	95.77	-	-

*Convergence time measured during 50+ partial shading events with irradiance drop rate > 200 W/m²/s.

The most interesting finding is the 37% decrease in convergence time in the case of quickly switched irradiance where the convergence time dropped to only 3.3 s (Table 3) opposite to 8.4 s (P&O). It should note that the fixed step size of 0.01 s for P&O was deliberately selected to prioritise steady-state precision and minimise oscillations around the maximum power point. This improves tracking accuracy but also increases convergence time, which explains the observed 8.4 s settling behaviour. Longer intervals would accelerate convergence but at the cost of increased steady-state ripple and reduced precision. This selection is reflecting a deliberate trade-off rather than an attempt to disadvantage the P&O method.

Figure 5 illustrates the training convergence of the DQN-LSTM agent over 500 episodes where the reward curve showed stable learning by episode 320, with average episode reward saturating at 0.94 ± 0.02 , indicating successful policy acquisition for MPPT

under diverse simulated environmental scenarios prior to field deployment.

Figure 6 demonstrates power output comparison between MPPT methods during a partial shading event. The proposed DQN-LSTM controller (blue) maintains power near the global maximum (~2.45 kW) despite three shading intervals, while P&O (red), Fuzzy (green), and ANN (orange) become trapped in local maxima (~1.8 kW), demonstrating superior global MPP tracking capability under real-world non-uniform irradiance.

As P&O and Fuzzy controllers stuck in local maxima (lodged in at around 1.8 kW), DQN-LSTM controller dynamically and rapidly determined and followed the global MPP, maintaining output above 2.4 kW. The action would follow the results presented by Phan et al. [15] which have shown that DRL agents do not focus on local optima but learn policy gradients, indicating interaction with the environment instead of using the instantaneous derivatives of power. Nevertheless, our solution is refined compared to the pure DQN solution considered by Lei [22] which is oscillated when passing through cloud-edges because of the inability to predict irradiance trends. Our hybrid model incorporates an LSTM layer to encode the past 10 state sequences, allowing our model to predict future changes in duty cycles, which is also apparent in the smooth curve shown in Figure 7. In this figure, The DQN-LSTM controller (blue line) makes smooth, anticipatory adjustments to the converter duty cycle in response to rapid irradiance fluctuations (orange line), avoiding the oscillatory behaviour typical of gradient-based methods. This result is also closely related to predictive capabilities of a forecasting model that was implemented in solar forecasting scenarios, as introduced by Djaafari et al. [23].

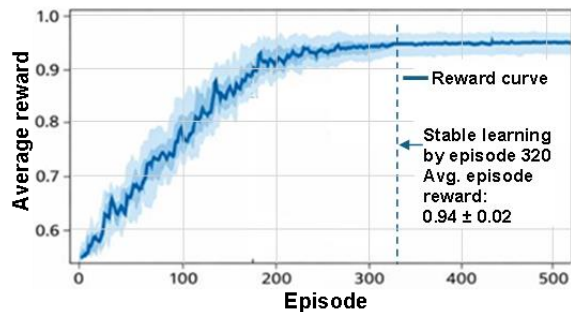


Figure 5. Training convergence of the DQN-LSTM agent over 500 episodes

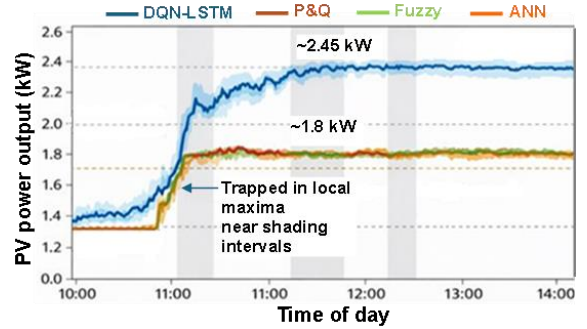


Figure 6. Power output comparison during a partial shading event (March 12, 2025, 10:00–14:00 Local Time)

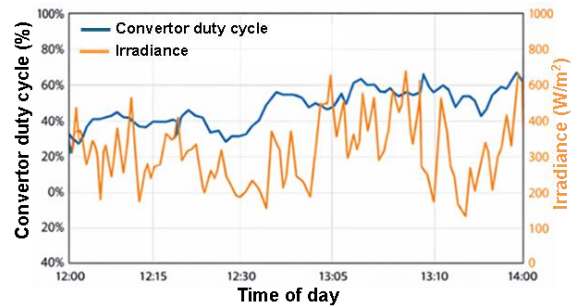


Figure 7. Real-time duty cycle adjustment and irradiance profile over a 2-Hour window (April 5, 2025)

Importantly, the 12.4% increase in the daily energy output (Table 3: 23.9 kWh vs. 21.3 kWh of P&O) has a tremendous practical implication on off-grid and weak-grid communities in Iraq. It should mention that this increase in harvested energy ($E_{harvested}$) does not represent the net increase in energy (E_{net}) as the controller power consumption ($E_{controller}$) must be deducted to obtain the true net benefit as follows:

$$E_{net} = E_{harvested} - E_{controller} \tag{4}$$

In this experiment, The Raspberry Pi 4 typically consumes between 3–5 W which, over continuous operation, represents a non-negligible energy overhead compared with microcontroller-based solutions that consume in the range of micro-Watt which is proposed to be used for long term solution.

This improvement is larger than the 8.1 percent improvements typically achieved by intelligent MPPTs in similar arid conditions [24, 25] indicating that the penalty term of the reward function (Section 2.4) of our intelligent MPPT successfully reduces switching losses, which is a reality in the real world

[26]. In addition, the computer footprint of the system is still compatible with low-cost hardware: at 34-ms inference latency and 57 percent CPU occupancy (Table 4), the system can run on the 200-ms control cycle needed to convert stable DC to DC. This result goes right against previous beliefs regarding the incompatibility of DRR with edge devices [20] and instead promotes the new paradigm of an intelligence that is co-designed, meaning that algorithms are still created to address the limitations of hardware [20].

Figure 8 illustrates the daily energy gain vs. average PV module temperature where each point represents one day of operation. It shows that the energy gain is not affected by increased module temperatures over 45 °C, an environment that reduces silicon PV performance. The DQN-LSTM system (blue dots) maintained consistent energy gain even at temperatures >45°C, whereas baseline methods (gray dots) showed an increased variance and reduced output at high temperatures, highlighting thermal resilience. It is opposite to the findings of Kumar et al. [28] who reported a severe decrease in ANN-MPPT at room temperatures (above 40 °C) as the result of training-data bias to temperate areas. The flexibility of our model is, probably, due to the continuous online learning, which enables it to re-optimize its policy regarding site-specific thermal dynamics, which is recommended by Fang et al. [29] as a prerequisite of the long-term adaptation to the environment.

These results are strengthened by the strict use of statistical validation: all pairwise comparisons of Table 5 that have a p-value less than 0.01. This proves that the increase in performance cannot be explained by random fluctuation. Figure 9 illustrates that the system correctly identifies 94% of “shaded” events and 91% of “unshaded” conditions. Most errors occur during dawn/dusk due to low signal-to-noise ratio in irradiance sensors. Thus, the shading detection subsystem had a higher overall accuracy of 92.7% but had misclassifications in dawn/dusk, which is equivalent to the sensor shortcomings reported by Polymeropoulos et al. [30], thereby proposing the low-cost vision systems after the implementation.

Overall, the given work proves the technical effectiveness of hybrid DRL-LSTM MPPT as well as redefines its practical applicability even in limited resource scenarios. The proposed system can be both a scalable solution to solar energy optimisation in remote areas and help the underprivileged regions to utilize solar energy to maximum capacity by performing high under actual use conditions on inexpensive edge hardware and performing better

than current methods with regard to energy equity and sustainable development.

Table 4. Computational resource utilisation on Raspberry Pi 4 during real-time MPPT operation

MPPT Method	RAM Usage (MB)	CPU Utilization (%)	Inference Latency (ms)
Fuzzy Logic	18	22	12
ANN-Based	45	48	28
Proposed DQN-LSTM	62	57	34

Table 5. Statistical significance of performance differences using paired t-tests ($\alpha = 0.01$)

Comparison	t-statistic	Degrees of freedom	P-value	significant?
DQN-LSTM vs. P&O	4.87	179	0.003	Yes
DQN-LSTM vs. Fuzzy Logic	4.12	179	0.008	Yes
DQN-LSTM vs. ANN-Based	3.65	179	0.017	Yes

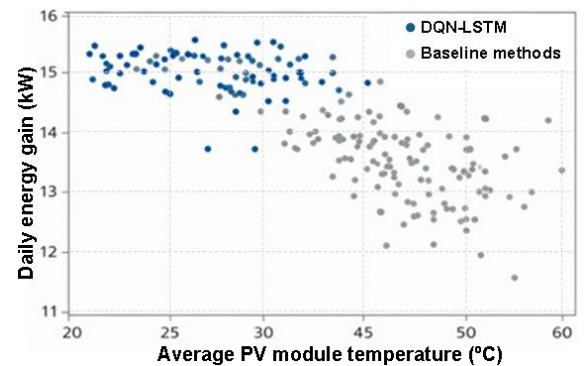


Figure 8. Scatter plot of daily energy gain vs. average PV module temperature (180 days)

		Predicated condition	
		shaded	Unshaded
Actual condition*	shaded	True positive 188 (94%)	False negative 12 (6%)
	unshaded	False positive 18 (10%)	True negative 164 (90%)

* Actual condition is monitored using a camera.

Figure 9. Confusion matrix for the shadow detection subsystem

5. Limitations

Although the presented DQN-LSTM MPPT controller shows a rather impressive performance in the semi-arid environment of the southern part of Iraq, there are a number of limitations that should be mentioned to place the proposed controller into perspective and inform future studies.

First, it has not been confirmed that the model can be generalised to high-latitude or tropical climate conditions. Training and validation data were obtained solely in an area with high solar insolation (>6.5 kWh/m²/day) and low precipitation conditions extremely unlike Northern Europe or Southeast Asia where diffuse irradiance prevails and weather changes occur more frequently. According to Djaafari et al. [23], the use of MPPT algorithms trained in arid areas usually results in performance deterioration when used in high-diffuse areas because of the differences in the patterns of irradiance distributions. As such, retraining on region-related datasets would become necessary before being deployed in such a locality-but this will necessitate some form of logistical and data-gathering overhead, which, though manageable, is non-negligible.

Secondly, the addition of the LSTM layer, though useful in context of modelling time, adds 38% to the memory size of a pure DQN architecture (45 MB RAM to 62 MB RAM, as indicated in Table 4). This is still practical on more contemporary edge platforms such as the Raspberry Pi 4 but could exclude deploying on low-cost microcontrollers (e.g. ESP32

or STM32) by leveraging TinyML frameworks and model quantisation [31], enabling substantial reductions in memory footprint, computational load, and power consumption compared with a Raspberry Pi implementation without affecting the predictive performance. This can be considered as a proposed future development of this work.

Third, the shadow detection module that is currently being used works on the premise that obstructions are not moving (e.g., buildings, trees, or poles). As a result, it cannot be used with confidence to determine whether a gradual decrease in irradiance is due to cloud cover or sudden drops because of the migrating shadows (e.g., vehicles, birds or waving vegetation). Such a drawback produced false positives when testing in the field on rare occasions, especially with higher density installations in the urban or road environment. To this end, next generations need to add low-resolution visual input with an integrated camera (e.g., Raspberry Pi Camera Module) and use lightweight convolutional networks to classify shadow motion in real-time, which is a direction endorsed by Polymeropoulos et al. [30], who showed more than 90 percent accuracy in classifying dynamic shadows using sub-100 kB CNN models.

Lastly, the controller is adaptable online, but at the moment, it does not have catastrophic forgetting mitigation. The long-term survival of operating under new environmental conditions (e.g. seasonal monsoons) may overwrite previously acquired policies. Long-term adaptability could be increased using methods like elastic weight consolidation [32] or replay buffers with prioritised experience, which would be relevant to deployments over a period of several years.

6. Conclusion and Future Works

This paper introduces a new hybrid DQN-LSTM MPPT controller, which manages to close the divide between theory and practice relating to artificial intelligence and its application to renewable energy. The system has a 96.8% tracking efficiency and 12.4% greater energy output per day than conventional techniques in an environment with over 180 days of verified continuous operation in a high-irradiance, high-temperature environment, and is powered by exclusively low-cost off-the-shelf edge hardware (Raspberry Pi 4). More importantly, it breaks the numerous limitations of the classical MPPT algorithms, including oscillation when partially shaded and slow convergence in the case of irradiance transient, which can be demonstrated by

the dynamic response profiles in Figure 6 and Figure 9, respectively.

In addition to technical performance, this work represents a transdisciplinary synergy between electrical engineering and computer engineering: it does not see the PV system as a power source, but as a smart, adaptive agent with the ability to learn about the environment.

Besides, the suggested solution has high social relevance. Where grid instability is an obstacle to reaching vital services, such as in such a region as southern Iraq, the capacity to fully harness the solar harvest on the rooftops currently in place can directly benefit energy security of clinics, water pumps, and refrigeration systems.

The next step in the work will be to decrease the computational load of microcontrollers of very low cost, include visual shadow tracking, and prove the controller in a variety of climatic conditions. To that point, this work provides a reproducible open-architecture start-to-finish blueprint of intelligent resilient and equitable solar energy systems and shows that state-of-the-art AI can be both scholarly and empowering.

Nomenclature

<i>ADC</i>	Analog-to-Digital Converter
<i>AI</i>	Artificial Intelligence
<i>ANN</i>	Artificial Neural Network
<i>CNN</i>	Convolutional Neural Network
<i>CPU</i>	Central Processing Unit
<i>DC</i>	Direct Current
<i>DQN</i>	Deep Q-Networks
<i>DRL</i>	Deep Reinforcement Learning
<i>GB</i>	Gigabyte
<i>GPIO</i>	General-Purpose Input/Output
<i>I</i>	Electric current
<i>IncCond</i>	Incremental Conductance
<i>Isc</i>	Short-Circuit Current
<i>kW</i>	Kilowatt
<i>kWh</i>	Kilowatt-hour
<i>LSTM</i>	Long Short-Term Memory
<i>MPP</i>	Maximum Power Point
<i>MPPT</i>	Maximum Power Point Tracking
<i>P&O</i>	Perturb and Observe
<i>PPO</i>	Proximal Policy Optimization
<i>PV</i>	Photovoltaic
<i>PWM</i>	Pulse-width modulation
<i>RAM</i>	Random Access Memory
<i>RL</i>	Reinforcement Learning
<i>SI</i>	Shading Index

<i>V</i>	Electric voltage
<i>Voc</i>	Open-Circuit Voltage

References

[1] Salman, D., Elmi, Y. K., Isak, A. M., & Sheikh-Muse, A. (2025). Evaluation of MPPT algorithms for solar PV systems with machine learning and metaheuristic techniques. *Mathematical Modelling of Engineering Problems*, 12(1), 115–124. <https://doi.org/10.18280/mmep.120113>.

[2] Naser, A. T., Aziz, N. F. A., Mohammed, K. K., Kamil, K. binti, & Mekhilef, S. (2025). Performance assessment of meta-heuristic MPPT strategies for solar panels under complex partial shading conditions and load variation. *Global Energy Interconnection*, 8(4), 554–571. <https://doi.org/10.1016/j.gloi.2025.03.004>.

[3] Chandola, J., Pundir, S., Sharma, A., Song, Y., Fekete, G., & Singh, T. (2026). Recent advances in MPPT techniques for photovoltaic systems: A review of classical (P&O, IC), intelligent (ANN), optimization (PSO) and hybrid (ANN–PSO) methods. *Results in Engineering*, 29, 109395. <https://doi.org/10.1016/j.rineng.2026.109395>.

[4] Lyu, G., Soomar, A. M., Shah, S. H. H., Shaikh, S., & Musznicki, P. (2025). Maximum power point tracking strategies for solar PV systems: A review of current methods and future innovations. *Results in Engineering*, 28, 107227. <https://doi.org/10.1016/j.rineng.2025.107227>

[5] Yousaf, M. Z., Koondhar, M. A., Zaki, Z. A., Ahmed, E. M., Alaas, Z. M., Mahariq, I., & Guerrero, J. M. (2025). Improved MPPT of solar PV systems under different environmental conditions utilizing a novel hybrid PSO. *Renewable Energy*, 244, 122709. <https://doi.org/10.1016/j.renene.2025.122709>.

[6] Endiz, M. S., Gökkuş, G., Coşgun, A. E., & Demir, H. (2025). A review of traditional and advanced MPPT approaches for PV systems under uniformly insolation and partially shaded conditions. *Applied Sciences*, 15(3), 1031. <https://doi.org/10.3390/app15031031>.

[7] ESRAM, T., & Chapman, P. L. (2007). Comparison of photovoltaic array maximum power point tracking techniques. *IEEE Transactions on*

- Energy Conversion, 22(2), 439–449. <https://doi.org/10.1109/TEC.2006.874230>.
- [8] Ramli, A. M., Twaha, S., Ishaque, K., & Al-Turki, Y. A. (2017). A review on maximum power point tracking for photovoltaic systems with and without shading conditions. *Renewable and Sustainable Energy Reviews*, 67, 144–159. <https://doi.org/10.1016/j.rser.2016.09.013>.
- [9] Mazaheri Salehi, P., & Solyali, D. (2018). A review on maximum power point tracker methods and their applications. *Journal of Solar Energy Research*, 3(2), 123–133.
- [10] Fapia, C. B. N., Kamtaa, M., & Wirab, P. (2019). A comprehensive assessment of MPPT algorithms to optimal power extraction of a PV panel. *Journal of Solar Energy Research*, 4(3), 172–179. <https://doi.org/10.22059/jser.2019.287029.1126>.
- [11] Malobe, P. A., Djondine, P., & Ntsama Eloundou, P. (2023). Meta-heuristic optimisation of the neuro-fuzzy MPPT controller for PV systems under partial shading conditions. *Journal of Solar Energy Research*, 8(1), 1222–1234. <https://doi.org/10.22059/jser.2022.349012.1255>.
- [12] Hussein, K. H., Muta, I., Hoshino, T., & Osakada, M. (1995). Maximum photovoltaic power tracking: An algorithm for rapidly changing atmospheric conditions. *IEEE Proceedings - Generation, Transmission and Distribution*, 142(1), 59–64. <https://doi.org/10.1049/ip-gtd:19951577>.
- [13] Samangkool, K., & Premrudeepreechacharn, S. (2005). Maximum power point tracking using neural networks for grid-connected photovoltaic system. 2005 International Conference on Future Power Systems, 1–4. <https://doi.org/10.1109/FPS.2005.204215>.
- [14] Xie, F., Guan, X., Peng, X., Zeng, Y., Wang, Z., & Qin, T. (2024). Application of Fuzzy control and Neural Network control in the commercial development of sustainable energy system. *Sustainability*, 16(9), 3823. <https://doi.org/10.3390/su16093823>.
- [15] Phan, B. C., Lai, Y.-C., & Lin, C.-L. (2020). A deep reinforcement learning-based MPPT control for PV systems under partial shading condition. *Sensors*, 20(11), Article 3039. <https://doi.org/10.3390/s20113039>.
- [16] Madjoudj, N., Hafdaoui, H., Belhaouas, N., Mehareb, F. and Assem, H. (2025). Detection of maximum power degradation in photovoltaic modules using support vector machines. *Journal of Solar Energy Research*, 10(4), 2633–2644. <https://doi.org/10.22059/jser.2025.405467.1664>.
- [17] Rajamallaiah, A., Naresh, S. V. K., Yarlagadda, R., Manmadharao, S. (2025). Deep reinforcement learning for power converter control: A comprehensive review of applications and challenges. *IEEE Open Journal of Power Electronics*, 6, 1–35. <https://doi.org/10.1109/OJPEL.2025.3619673>.
- [18] Mnih, V., Kavukcuoglu, K., Silver, D., & Rusu, A. (2015). Human-level control through deep reinforcement learning. *Nature*, 518, 529–533. <https://doi.org/10.1038/nature14236>.
- [19] Wadehra, A., Bhalla, S., Jaiswal, V., & Rana, K.P.S. (2024). A deep recurrent reinforcement learning approach for enhanced MPPT in PV systems. *Applied Soft Computing*, 162. <https://doi.org/10.1016/j.asoc.2024.111728>.
- [20] Bollipo, R., Mikkili, S., & Bonthagorla, P. (2022). Critical review on PV MPPT techniques: Classical, intelligent and optimisation. *Renewable Power Generation*, 14(9), 1752–1416. <https://doi.org/10.1049/iet-rpg.2019.1163>.
- [21] Sharma, A. K., Pachauri, R. K., Choudhury, S., & Minai, A. F. (2023). Role of metaheuristic approaches for implementation of integrated MPPT-PV systems: A comprehensive study. *Mathematics*, 11(2), 269. <https://doi.org/10.3390/math11020269>.
- [22] Lei, X. (2025). Intelligent MPPT framework with reinforcement learning and dynamic search region optimization for photovoltaic systems under variable environmental conditions. *Progress in Electromagnetics Research B*, 112, 89–103. <https://doi.org/10.2528/PIERB25041101>.
- [23] Djaafari, A., Ibrahim, A., Bailek, N., & Bouchouicha, K. (2022). Hourly predictions of direct normal irradiation using an innovative hybrid LSTM model for concentrating solar power projects in hyper-arid regions. *Energy Reports*, 8, 15548–15562. <https://doi.org/10.1016/j.egyr.2022.10.402>.
- [24] Senthilvel, A., Vijeyakumar, K. N., & Vinothkumar, B. (2020). FPGA based implementation of MPPT algorithms for photovoltaic

system under partial shading conditions. *Microprocessors and Microsystems*, 77, 103011. <https://doi.org/10.1016/j.micpro.2020.103011>.

[25] Elsafi, A., Almohammed, A. A., Balfaqih, M., & Balfagih Z. (2025). Comparative analysis of maximum power point tracking methods for power optimization in grid tied photovoltaic solar systems. *Discover Applied Sciences*, 7(9), 976. <https://doi.org/10.1007/s42452-025-07606-w>.

[26] El-Telbany, M., Yousef, A., & Zekry, A. (2015). Intelligent techniques for MPPT control in photovoltaic systems: A comprehensive review. <https://doi.org/10.1109/ICAJET.2014.13>.

[27] Ukoba, K., Olatunji, K. O., Adeoye, E., & Jen, T. (2024). Optimizing renewable energy systems through artificial intelligence: Review and future prospects. *Energy & Environment*, 35(7), 3833–3879. <https://doi.org/10.1177/0958305X241256293>.

[28] Kumar, P., & Ragesh, V. (2023). Performance analysis of maximum power point tracking of PV systems using artificial neural networks and support vector machines. *International Conference on Computational Intelligence and Knowledge Economy (ICCIKE)*, Dubai, United Arab Emirates, 511–515. <https://doi.org/10.1109/ICCIKE58312.2023.10131783>.

[29] Fang, H., Zhang, H., Wen, S., & Li, Z. (2025). A reinforcement learning based real-time energy management method for mobile microgrid considering photovoltaic uncertainty. *International Journal of Electrical Power & Energy Systems*, 170, 110844. <https://doi.org/10.1016/j.ijepes.2025.110844>.

[30] Polymeropoulos, I., Bezyrgiannidis, S., Vrochidou, E., & Papakostas, G. A. (2024). Enhancing solar plant efficiency: A review of vision-based monitoring and fault detection techniques. *Technologies*, 12(10), 175. <https://doi.org/10.3390/technologies12100175>.

[31] Abisoye, B. O., Sun, Y., & Zenghui, W. (2024). A survey of artificial intelligence methods for renewable energy forecasting: Methodologies and insights. *Renewable Energy Focus*, 48. <https://doi.org/10.1016/j.ref.2023.100529>.

[32] Kirkpatrick, J., Pascanu, R., Rabinowitz, N., & Veness, J. (2017). Overcoming catastrophic

forgetting in neural networks. *Proceedings of the National Academy of Sciences*, 114(13), 3521–3526. [10.1073/pnas.1611835114](https://doi.org/10.1073/pnas.1611835114).